

Electronic stopping power calculation method for Molecular Dynamics simulations using local Firsov and free-electron-gas models.

J. Peltola*, K. Nordlund and J. Keinonen

Accelerator Laboratory, P.O. Box 43, FIN-00014 University of Helsinki, Finland

(May 24, 2006)

Abstract

Molecular dynamics simulations have proven to be accurate in predicting depth distributions of low-energy ions implanted in materials. Free parameters adjusted for every ion-target combination are conventionally used to obtain depth profiles in accordance with the experimental ones. We have previously developed a model for predicting depth profiles in crystalline Si without free parameters. The electronic stopping power was calculated using local total electron density. The model underestimated the stopping in the $\langle 110 \rangle$ channeling direction. We have now taken a new approach to calculate the electronic stopping power. We use the local valence ($3p^2$) electron density to account for the electronic energy loss between collisions and the Firsov model to account for the electronic energy loss during collision. The lowest electron densities are adjusted with a parametrization that is the same for all ions in all implanting directions to correct the problems in the $\langle 110 \rangle$

*Corresponding author: Jarkko Peltola, Accelerator Laboratory, P.O. Box 43, FIN-00014 University of Helsinki, Email jypeltol@acclab.helsinki.fi, phone +358-9-19150003, fax +358-9-19150042

channeling direction.

I. INTRODUCTION

Calculating the force which slows down energetic ions traversing in materials (the stopping power) is a long-standing problem of considerable theoretical and practical interest¹⁻³. While the stopping power caused by collisions between an ion and atoms can now be predicted very accurately⁴⁻⁶, there is still an uncertainty in how the stopping caused by collisions between an ion and electrons (electronic stopping) should be calculated for ion velocities below the Bohr velocity (namely at energies of the order of 0.1 - 10 keV/amu). This is an especially pressing problem for obtaining range profiles for dopants implanted in crystal channel directions in semiconductors, since on the one hand the uncertainties are particularly large in this case, and on the other hand this case is important for the microelectronics industry.

Several computer models have been developed for predicting depth profiles of implanted ions in silicon. These codes fall into two categories based on how they calculate the interactions between the atoms: models using Binary Collision Approximation (BCA)⁷⁻¹⁰ and models using the Molecular Dynamics (MD) method^{11,12,5}. In BCA codes, the interactions are treated as two-body collisions and the energy loss of the colliding ion is determined by the impact parameter. In the MD method, the energy loss of the ion is calculated by using many-body-interactions and the information of the local electron environment. Thus it is more accurate in predicting the range profiles for low energies¹³. In both methods a free parameter is used to adjust the simulated concentration profiles to match the experimental ones. This weakens the predictive power of the codes. Our previous models^{14,15} have been developed without free parameters. This has given good overall results for calculating the stopping power of crystalline Si (c-Si) in all channel directions except the $\langle 110 \rangle$ channel. The development of the MD method in ion implantation simulations is important, because it leaves room for adding more complex phenomena, e.g. cluster implantation, to the simulations without unnecessary approximations or parametrizations.

In this paper, we present a new model for calculating the electronic stopping power for a given ion in c-Si. The improvement over the previous model is done by calculating the energy loss due to the momentum exchange between the ion and the electrons in the target

using the valence ($3p^2$) electron density and using a separate model for electronic energy loss during close collisions between the ion and atom in the target. A single free parameter valid for all implantations in Si is introduced to correct the problems of the previous model in the $\langle 110 \rangle$ direction. We compare the results with a wide range of experimental range profiles for implantation in silicon channels. Comparison to the results of other models is not given because models by others adjust different parameter sets for each ion-atom combination^{5,16}, thus having the capability to produce arbitrarily good results for any implantation case. The deviation of the simulated concentration profile from the experimental one can be up to 100 % with the state-of-the-art codes^{16,5,17}, some using several free parameters. This sets the scale for the goodness of the simulation results.

II. ELECTRONIC STOPPING MODEL

In our previous model¹⁵, the electronic stopping S_{ech} was calculated using a model based on the Density Functional Theory (DFT) calculations for a static ion in a free electron gas^{18,19}:

$$S_{\text{Ech}} = \frac{3v}{k_F r_s^3} \sum_{l=0}^{\infty} (l+1) \sin^2(\delta_l(E_F) - \delta_{l+1}(E_F)), \quad (1)$$

where v is the ion velocity, $r_s = (4\pi n/3)^{-1/3}$ is the one-electron-radius and $\delta_l(E_F)$ is the phase-shift values for an electron scattering from the Fermi surface. In the simulations, the electron number density n of the gas was taken from a 3-dimensional electron distribution²⁰ for a c-Si unit cell. The 3D density used was the local total electron density, which includes also the core electrons. This is in contradiction to the free electron gas picture which the eq. (1) is based on.

The calculation procedure of the 3D density allows partitioning the electron distribution to the core electrons and the valence electrons²¹. The reason behind this fact is that there is a significant energy separation in the band structure between core and valence states in Si. Thus we can subtract the core electrons (1s, 2s, 2p) from the density profile. We can also subtract the 3s electrons, which leaves us the valence density of most loosely bound electrons 3p, which is physically more appealing to be used as the free-electron gas density required by eq. (1). We calculated the valence ($3p^2$) electron density profile of the Si unit cell, which

gave us the local density of these electrons inside the Si crystal. Phase-shifts were calculated with DFT for each ion and for a grid of electron density values. In the simulations, eq. (1) was used for each value of v and n to take into account the momentum exchange between the potential of the ion and the electron gas.

The low energy ion has its own electron shells filled and in close collisions with the target atoms the electron clouds interact. This leads to a contribution to the electronic stopping of the ion which can be approximated by the Firsov model. We include the Firsov model by using the approach derived by Elteckov *et al.*²², where the slowing force (in Newtons) is given by

$$F(R, v) = \frac{-0.7h}{(\pi a_b)^2} \left[\frac{Z_A^2}{(1 + 0.8\alpha Z_A^{1/3} R/a)^4} + \frac{Z_B^2}{(1 + 0.8(1 - \alpha) Z_B^{1/3} R/a)^4} \right] v \text{ N}, \quad (2)$$

where a_b is the Bohr radius, $a = 0.47 \text{ \AA}$, Z_A and Z_B ($Z_A > Z_B$) are the atomic numbers of the colliding atoms and $\alpha = 1 / [1 + (Z_B/Z_A)^{1/6}]$. In our previous model¹⁵ the Firsov model was not utilized. The Firsov model takes into account the electronic energy loss due to the electron exchange between the ion and the atoms in the target thus taking into account the valence $3p$ electrons of the target also. The Firsov model alone clearly underestimates the electronic stopping for the ions in channeling conditions. We found out that the model with Firsov formulae and the use of only $3p$ electron density in eq. 1 improved the agreement with the experimental profiles in all implantation directions except in the $\langle 110 \rangle$ direction, giving the same or slightly stronger stopping values than the previous model. If the $3s$ valence electrons were also included in the electron density in the new model, the total electronic stopping was too strong, clearly worsening the agreement with the experiments. These results imply that utilizing eq. 2 compensates almost exactly the neglect of the other electrons than $3p$ from the density value used in eq. 1. This means that the possible double count of the $3p$ electron contribution is rather an empirically motivated correction to eq. 2 than a serious misuse of these models. This separation of the models gives us better physical motivation for the calculation of the electronic stopping, instead of the controversy of using total electron density in eq. 1.

In our previous model, the long channeling tails of the depth profiles, especially in the

$\langle 110 \rangle$ direction of Si, were a result of the point-like ion travelling along the open channel and thus experiencing a very low electron density. We found that the lower electron densities could be changed to some extent, to suppress the channeling tails in the $\langle 110 \rangle$ direction, but not in the profiles in other directions. The total electron density varies over 5 decades in Si, so the increase in the lowest densities has no effect on the total amount of charge in the crystal. We used a parameterization that raises the electron density n by a factor of $n_a(n) = n * k(n_c - n)^2$ if $n < n_c$, where n_c is an adjustable limiting value and k is the strength of the increase. There are two adjustable parameters, which require two conditions. We adjusted the parameters n_c and k so that the simulated $\langle 110 \rangle$ profile of the 15 keV B ions (Fig. 2) matches to the experimental profile and that the $\langle 100 \rangle$ profile of the 15 keV B ions is not affected by the parametrization. We chose these particular cases for adjusting the parametrization, because the simulated profiles of the 15 keV B ions were in a good agreement with the experiments in random and $\langle 100 \rangle$ directions¹⁵. The first condition ($\langle 110 \rangle$) gives the value for the k and the second ($\langle 100 \rangle$) for the n_c . k is referred to as a free parameter in this paper because it can be used to adjust the length of the channeling tails directly. The parameter optimization gave us $n_c = 0.06 \text{ e}/\text{\AA}^3$ and $k = 3188 \text{ (e}/\text{\AA}^3)^{-2}$. The effect of this parametrization can be seen in Fig. 1.

We emphasize that we do not think there is anything wrong *per se* with the 3D electron density of Deutsch²¹, especially since a very similar density has also been reported by others²³. Instead the physical motivation of our modification is to make an effective compensation for the use of the local electron density of a *point-like* ion. Since at these velocities the ions are not stripped of electrons, they are not pointlike but experience an electron density averaged over a somewhat larger volume. Hence raising the electron density is effectively the same as averaging over a larger sample region. But doing this is only needed in the $\langle 110 \rangle$ channel, since this is the only direction for which the ion never experiences high electron densities.

III. SIMULATION RESULTS

We used the MDRANGE²⁴ code developed in our laboratory to simulate depth profiles in crystalline Si for B, As, P and Al ions. The depth profile of implanted ions is calculated as a histogram of the travelling distances from the surface projected to the implantation direction. 5000 ions were simulated for each case. Thermal displacements at 300 K were included for target atoms, corresponding to the measured Debye temperature of 519 K²⁵. The surface oxide was simulated by an amorphous layer (16Å) of Si and O atoms on the top of c-Si. A ZBL² electronic stopping was used for the ions in the oxide layer. The points of impacts are distributed randomly over the unit cell area. The incident angle is determined as the polar angle θ between the surface normal (001) and the ion velocity and the azimuthal angle ϕ around the surface normal. The simulations in the random direction were done by giving the ions an incident angle of ($\theta = 6^\circ - 8^\circ$, $\phi = 0^\circ - 360^\circ$) taking into account an angular deviation of 1° . In the channeling directions the incident angles were ($0^\circ - 360^\circ$, $0^\circ - 1^\circ$) for the $\langle 100 \rangle$ direction, (0° , $44^\circ - 46^\circ$) for the $\langle 110 \rangle$ direction and (45° , $54^\circ - 56^\circ$) for the $\langle 111 \rangle$ direction.

We call the results from the previous model, which uses the total electron density without the Firsov model, the “old model” in the figures. The changes between the new and the old model in simulated profiles in the $\langle 110 \rangle$ direction presented are mostly due to the free parameter. The $n_a(n)$ was so small that the simulated profiles in other directions than $\langle 110 \rangle$ were affected slightly (few nanometers at maximum), but most of the changes in those directions resulted from the combined use of valence ($3p^2$) density and the Firsov model.

The statistics in the profiles is more accurate for the new model as compared to the old one because we have used a REED⁵ algorithm with the new model. The REED algorithm divides the simulated ions to virtual ions thus keeping the statistics at the same level for every concentration level. The error bars are marked only in Fig. 2 to show the magnitude of the statistical error. We have not included error bars in other figures to keep them clear. The fluctuations in the simulated profiles are of about the same magnitude as the statistical error.

A. B ions

Fig. 2 shows the simulated ranges of 15 keV B ions in the $\langle 110 \rangle$ direction with both models as compared to the experiments. This case was used to optimize the free parameter, so the excellent agreement with the experiments is understandable. Fig. 3 shows the simulations of 15 keV and 80 keV B ions in the $\langle 100 \rangle$ direction as compared to the experiments. The new model gives approximately the same results as the old model. This shows how the use of $n_a(n)$ shortens the channeling tails significantly (maximum ranges are decreased by 40 - 50 %) in the $\langle 110 \rangle$ direction but does not affect much the profiles in the $\langle 100 \rangle$ direction.

B. P ions

Fig. 4 shows the simulated and the experimental profiles of the 100 keV P implanted in a random direction. The results of the new model are in a slightly better agreement with the experiments than the old model results. Fig. 5 shows the simulated and the experimental profiles for 15, 50 and 200 keV P ions in the $\langle 100 \rangle$ channeling direction. The channeling tails in the results of the old model have been reduced in the new model, which gives good results as compared to the experiments. The simulation results for the range profiles of 50 and 100 keV P ions in the $\langle 110 \rangle$ direction are in decent agreement with the experiments as shown in Fig. 6. The channeling tails of the old model profiles are significantly reduced. Fig. 7 shows the results for 50 keV P in the $\langle 111 \rangle$ direction. The new model gives again better results compared to the experiments and shorter channeling tails than the old model. The reduction of the tails in the $\langle 100 \rangle$ and $\langle 111 \rangle$ directions results from the use of the Firsov model, not from the parametrization as in the $\langle 110 \rangle$ direction.

C. As ions

Fig. 8 shows the simulated and the experimental depth profiles of 100 keV As ions implanted in the random direction. The new model gives the same results as the old model and both of them are in a good agreement with the experiment. The results for As ions

implanted in the $\langle 100 \rangle$ direction with energies of 50 and 180 keV are shown in Fig. 9. The results show that the simulation with the new model gives very good results for the 50 keV case. The channeling tail is again reduced for both energies. Fig. 10 shows the results in the $\langle 110 \rangle$ direction for implantations of 75 and 150 keV As ions. The results show the same behavior as for the P ions in Fig. 6.

D. Al ions

Fig. 11 shows the simulated and the experimental profiles for the 80 keV Al ions implanted in the random direction. The new model gives approximately the same results as the old model, slightly reducing the tail of the profile. The results are in a good agreement with the experiments. Fig. 12 shows the results in the $\langle 110 \rangle$ direction for 150 keV ions with two different sets of experiments, one measured using differential capacitance-voltage (C-V) profiling and one using SIMS. The channeling tail is reduced with the new model but not so much as for the P or As ions. The results show that the old model is in a slightly better agreement with the experiments than the new model.

IV. DISCUSSION AND CONCLUSIONS

We have developed a new model for calculating the local electronic stopping power in MD simulations. The electronic stopping was calculated using the valence ($3p^2$) electron density profile of the crystalline Si and the DFT -based model for the free-electron gas electronic energy loss. The in-collision contribution was calculated using a model by Firsov. Our simulations show that the use of these stopping models gives too long channeling tails in the range profile in the $\langle 110 \rangle$ direction. There must be an additional contribution that increases the stopping experienced by the ion in the most open channel of c-Si, the $\langle 110 \rangle$ channel. We have accounted for this by using a free parameter, which raises the electron density experienced by the ion in the regions of lowest density e.g. in the $\langle 110 \rangle$ channel. This affected only slightly the profiles in the other directions. The same free parameter is used for all the ion species. The new model gives very good results in the random direction for all the ions presented in this paper. The results in the $\langle 100 \rangle$ and $\langle 111 \rangle$ directions show

a good agreement and in the $\langle 110 \rangle$ direction a decent agreement with the experiments for all the ions. The simulations show that the depth profiles of Al have overall longer channeling tails as compared to the other ions.

There are still discrepancies with experiments in the channeling directions: the channeling peaks in the $\langle 110 \rangle$ direction are not reproduced as well as the random peaks and the slopes of the simulated channeling profiles get worse, when the energy is increased. Reasons affecting the discrepancies in the slope and channeling peaks are related to the electronic stopping model used. This has become clear by looking at the simulation results of range profiles in amorphous²⁶ and randomly oriented structures presented in this paper. The shape of the simulated channeling peak can be changed just by adjusting the electron density differently, which also shows that the problem is related to the modelling of the electronic stopping.

We conclude that our new model for the calculation of the local electronic stopping is physically better motivated than the old model and gives results which are in a better agreement with experiments.

ACKNOWLEDGMENTS

The research was supported by the Academy of Finland under projects No. 44215 and 46788. Generous grants of computer time from the Center for Scientific Computing in Espoo, Finland are gratefully acknowledged.

REFERENCES

- ¹ N. Bohr, *Phil. Mag.* **25**, 10 (1913).
- ² J. F. Ziegler, J. P. Biersack, and U. Littmark, *The Stopping and Range of Ions in Matter* (Pergamon, New York, 1985).
- ³ D. F. Downey, C. M. Osburn, and S. D. Marcus, *Solid State Technology* **40**, 71 (1997).
- ⁴ K. Nordlund, J. Keinonen, and A. Kuronen, *Physica Scripta* **T54**, 34 (1994).
- ⁵ K. M. Beardmore and N. Grønbech-Jensen, *Phys. Rev. E* **57**, 7278 (1998).
- ⁶ K. Nordlund, N. Runeberg, and D. Sundholm, *Nucl. Instr. Meth. Phys. Res. B* **132**, 45 (1997).
- ⁷ M. Hautala, *Phys. Rev. B* **30**, 5010 (1984).
- ⁸ M. T. Robinson and I. M. Torrens, *Phys. Rev. B* **9**, 5008 (1974).
- ⁹ Q. Yang, T. Li, B. V. King, and R. J. MacDonald, *Phys. Rev. B* **53**, 3032 (1996).
- ¹⁰ K. M. Klein, C. Park, and A. F. Tasch, *IEEE Trans. Electron Devices* **39**, 1614 (1992).
- ¹¹ J. Keinonen *et al.*, *Phys. Rev. Lett.* **67**, 3692 (1991).
- ¹² K. Nordlund, *Comput. Mater. Sci.* **3**, 448 (1995).
- ¹³ G. Hobler and G. Betz, *Nucl. Instr. Meth. Phys. Res. B* **180**, 203 (2001).
- ¹⁴ J. Sillanpää, K. Nordlund, and J. Keinonen, *Phys. Rev. B* **62**, 3109 (2000).
- ¹⁵ J. Sillanpää *et al.*, *Phys. Rev. B* **63**, 134113 (2000).
- ¹⁶ S. Tian, *J. Appl. Phys.* **93**, 5893 (2003).
- ¹⁷ J. M. Hernandez-Mangas *et al.*, *Solid-State Electronics* **46**, 1315 (2002).
- ¹⁸ J. Finneman, dissertation, The Institute of Physics, Aarhus, 1968 (unpublished).
- ¹⁹ T. L. Ferrell and R. H. Ritchie, *Phys. Rev. B* **16**, 115 (1977).
- ²⁰ M. Deutsch, *Phys. Rev. B* **45**, 646 (1992), **46** 607 (1992).

- ²¹ Z. W. Lu, A. Zunger, and M. Deutsch, Phys. Rev. B **47**, 9385 (1993).
- ²² V. A. Elteckov, D. S. Karpuzov, Y. V. Martynenko, and V. E. Yurasova, in *Atomic Collision Phenomena in Solids*, edited by D. Palmer, M. W. Thompson, and P. D. Townsend (North-Holland, Amsterdam, 1970), Chap. ion penetration into Si single crystal, p. 657.
- ²³ J. A. Golovchenko, D. E. Cox, and A. N. Goland, Phys. Rev. B **26**, 2335 (1982).
- ²⁴ A presentation of the MDRANGE computer code is available on the World Wide Web in
http://beam.helsinki.fi/~knordlun/mdh/mdh_program.html .
- ²⁵ G. Buschorn *et al.*, Phys. Rev. B **55**, 6196 (1997).
- ²⁶ J. Peltola, K. Nordlund, and J. Keinonen, Nucl. Instr. Meth. Phys. Res. B **195**, 269 (2002).
- ²⁷ D. Cai, N. Grønbech-Jensen, C. M. Snell, and K. M. Beardmore, Phys. Rev. B **54**, 17147 (1996).
- ²⁸ D. Cai, C. M. Snell, K. M. Beardmore, and N. Grønbech-Jensen, International J. Modern Physics C **9**, 459 (1998).
- ²⁹ R. Wilson, J. Appl. Phys **60**, 2797 (1986).
- ³⁰ R. G. Wilson, J. Appl. Phys. **52**, 3985 (1980).
- ³¹ G. Galvagno *et al.*, Nucl. Instr. Meth. Phys. Rev. B **74**, 105 (1993).

FIGURES

FIG. 1. Effect of the modification of the valence ($3p^2$) electron density along the $\langle 111 \rangle$ direction of a Si crystal. The two atom positions show up as high peaks in the profiles. In the modified electron density curve, the electron density is raised by a function described in the text when the density is lower than $n_c = 0.06 \text{ e}/\text{\AA}^3$. This shows up as a higher electron density in the “valley” which is the $\langle 110 \rangle$ channel.

FIG. 2. Simulated and measured ranges of 15 keV B ions in the $\langle 110 \rangle$ channel of silicon. The error bars in the simulated profiles are shown as to present the magnitude of the statistical error. The experimental data were measured with SIMS (Ref.²⁷).

FIG. 3. Simulated and measured ranges of 15 and 80 keV B ions in the $\langle 100 \rangle$ channel of silicon. The experimental data were measured with SIMS (Ref.²⁷).

FIG. 4. Simulated and measured ranges of 100 keV P ions in the random direction of silicon. The experimental data were measured with SIMS (Ref.²⁸).

FIG. 5. Simulated and measured ranges of 15, 50 and 200 keV P ions in the $\langle 100 \rangle$ channel of silicon. The experimental data were measured with SIMS (Ref.^{28,29}).

FIG. 6. Simulated and measured ranges of 50 and 100 keV P ions in the $\langle 110 \rangle$ channel of silicon. The experimental data were measured with SIMS (Ref.²⁹).

FIG. 7. Simulated and measured ranges of 50 keV P ions in the $\langle 111 \rangle$ channel of silicon. The experimental data were measured with SIMS (Ref.²⁹).

FIG. 8. Simulated and measured ranges of 100 keV As ions in the random direction of silicon. The experimental data were measured with SIMS⁵

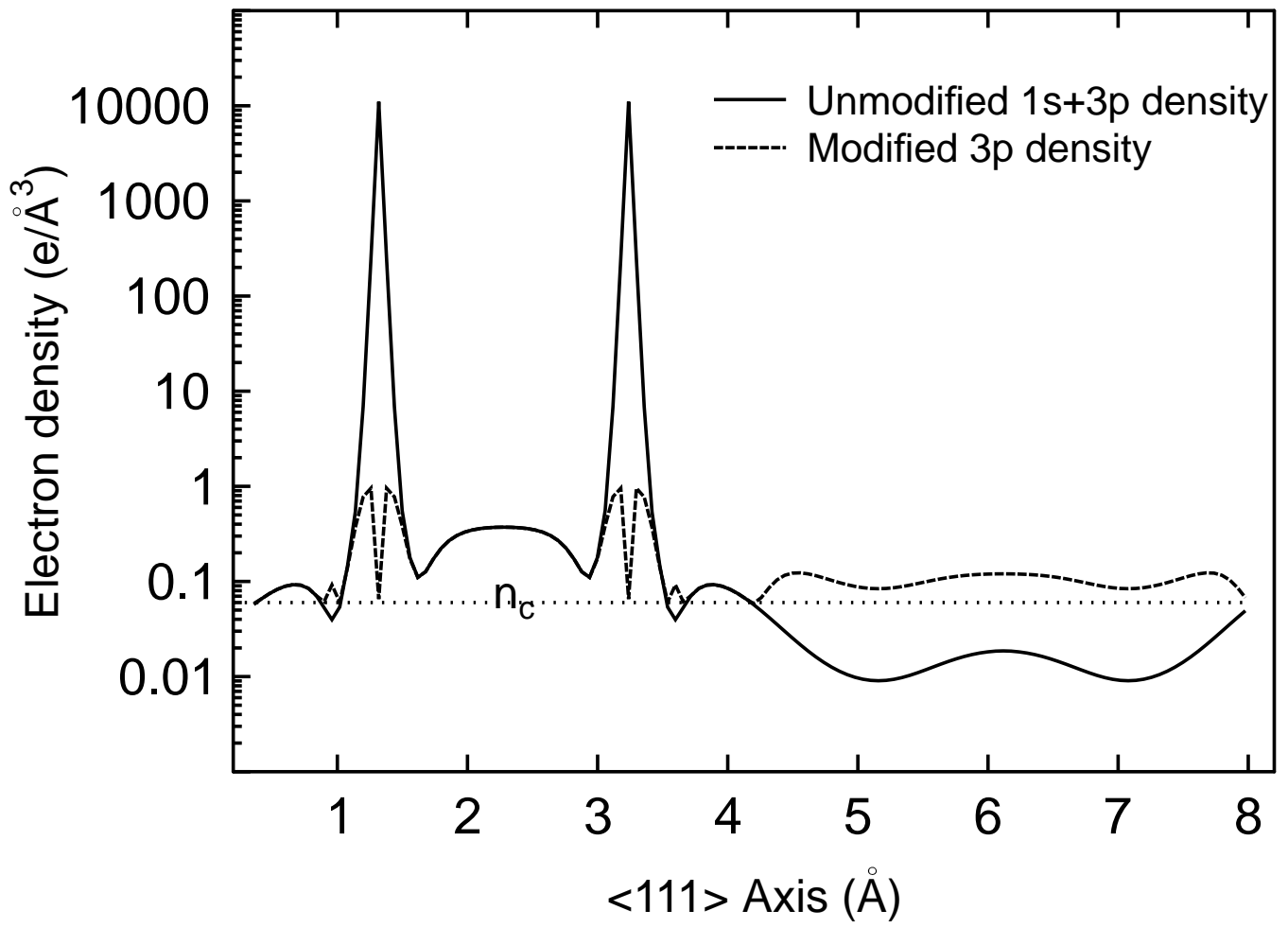
FIG. 9. Simulated and measured ranges of 50 keV and 180 keV As ions in the $\langle 100 \rangle$ channel of silicon. The experimental data were measured with SIMS (Ref.²⁷).

FIG. 10. Simulated and measured ranges of 75 keV and 150 keV As ions in the $\langle 110 \rangle$ channel of silicon. The experimental data were measured with SIMS (Ref.³⁰).

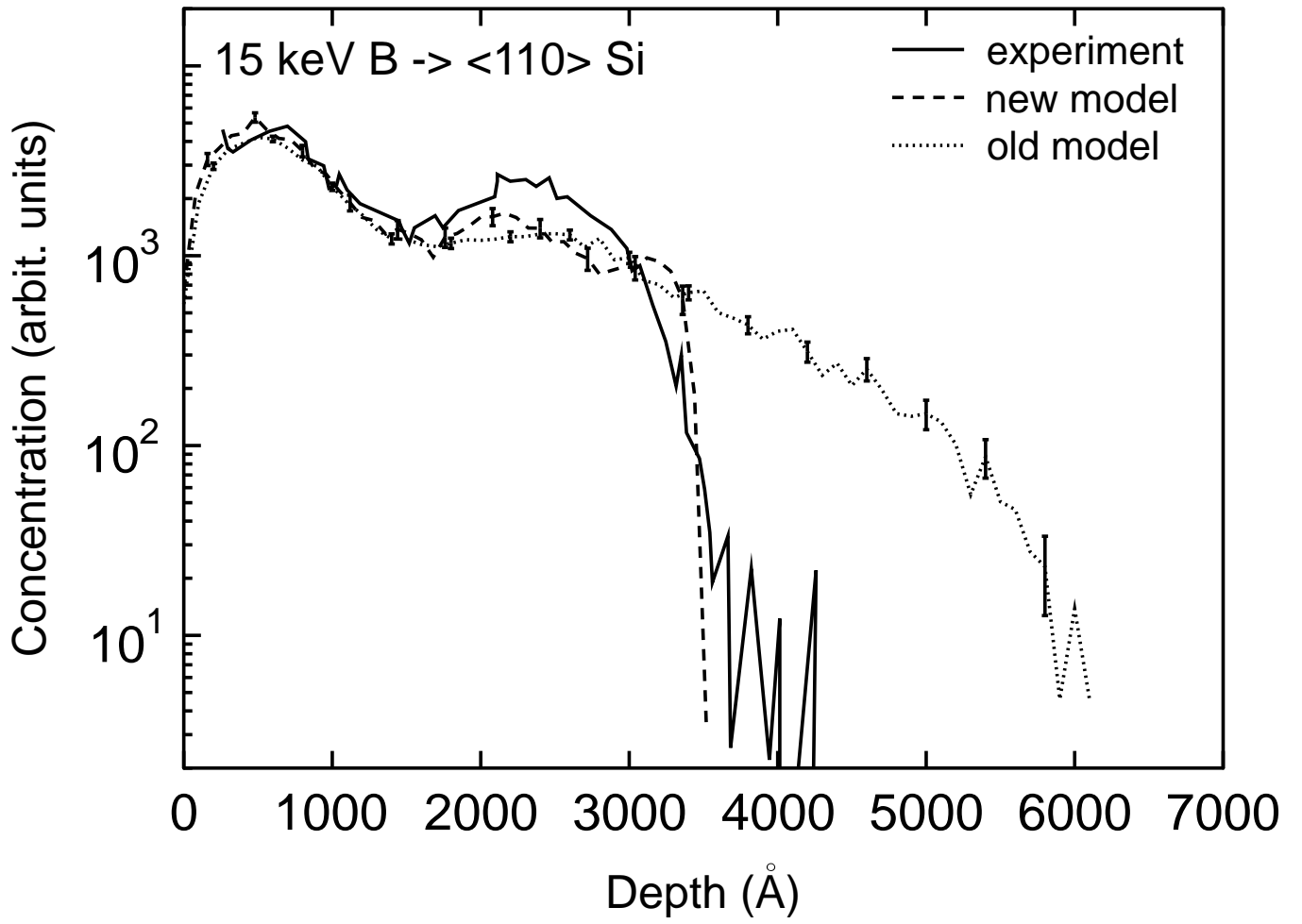
FIG. 11. Simulated and measured ranges of 80 keV Al ions in the random direction of silicon. The experimental data were measured with SIMS³¹

FIG. 12. Simulated and measured ranges of 150 keV Al ions in the $\langle 110 \rangle$ channel of silicon. The experimental data were measured with SIMS and C-V (Ref.²⁹).

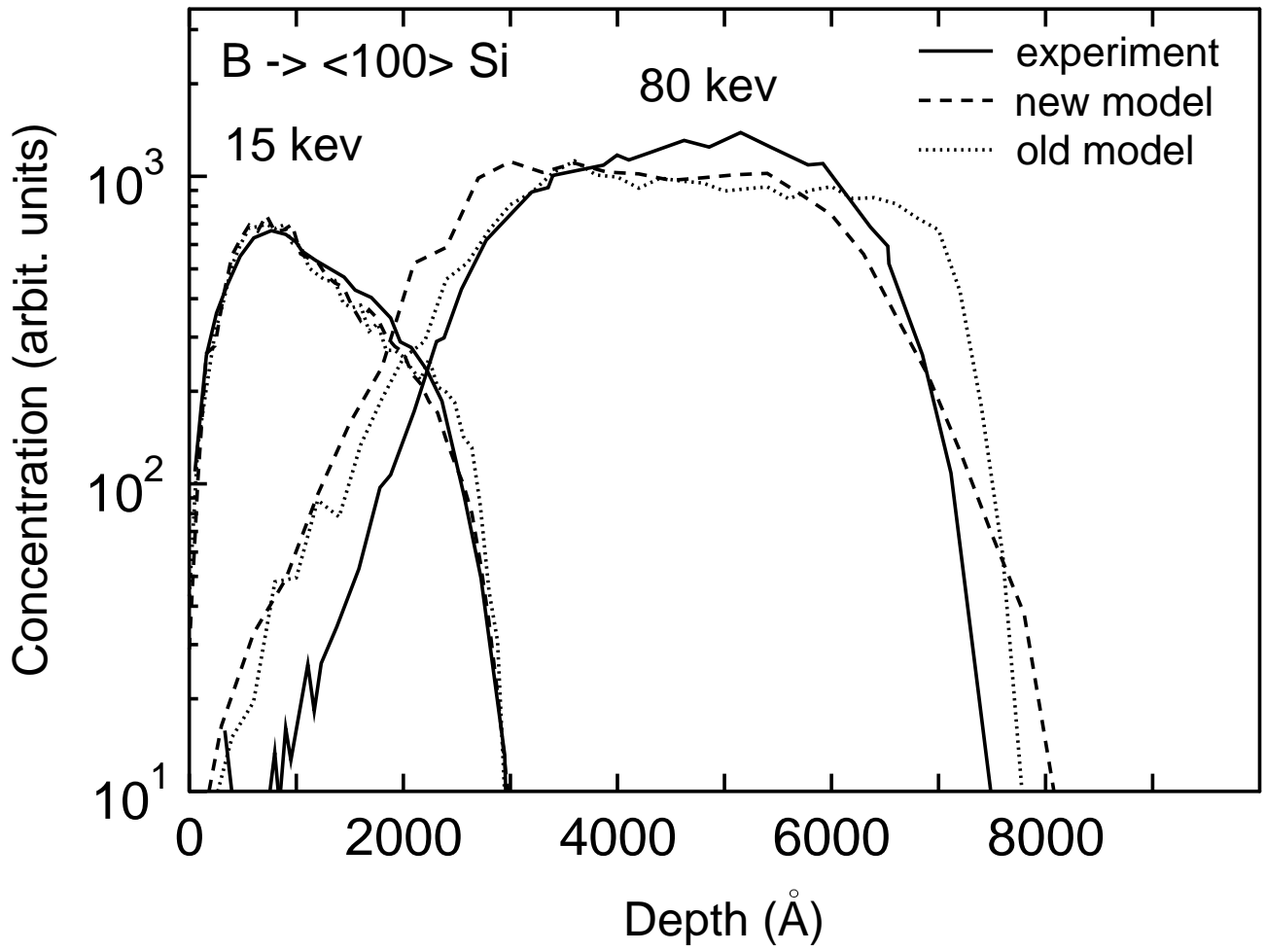
Peltola Fig. 1/12



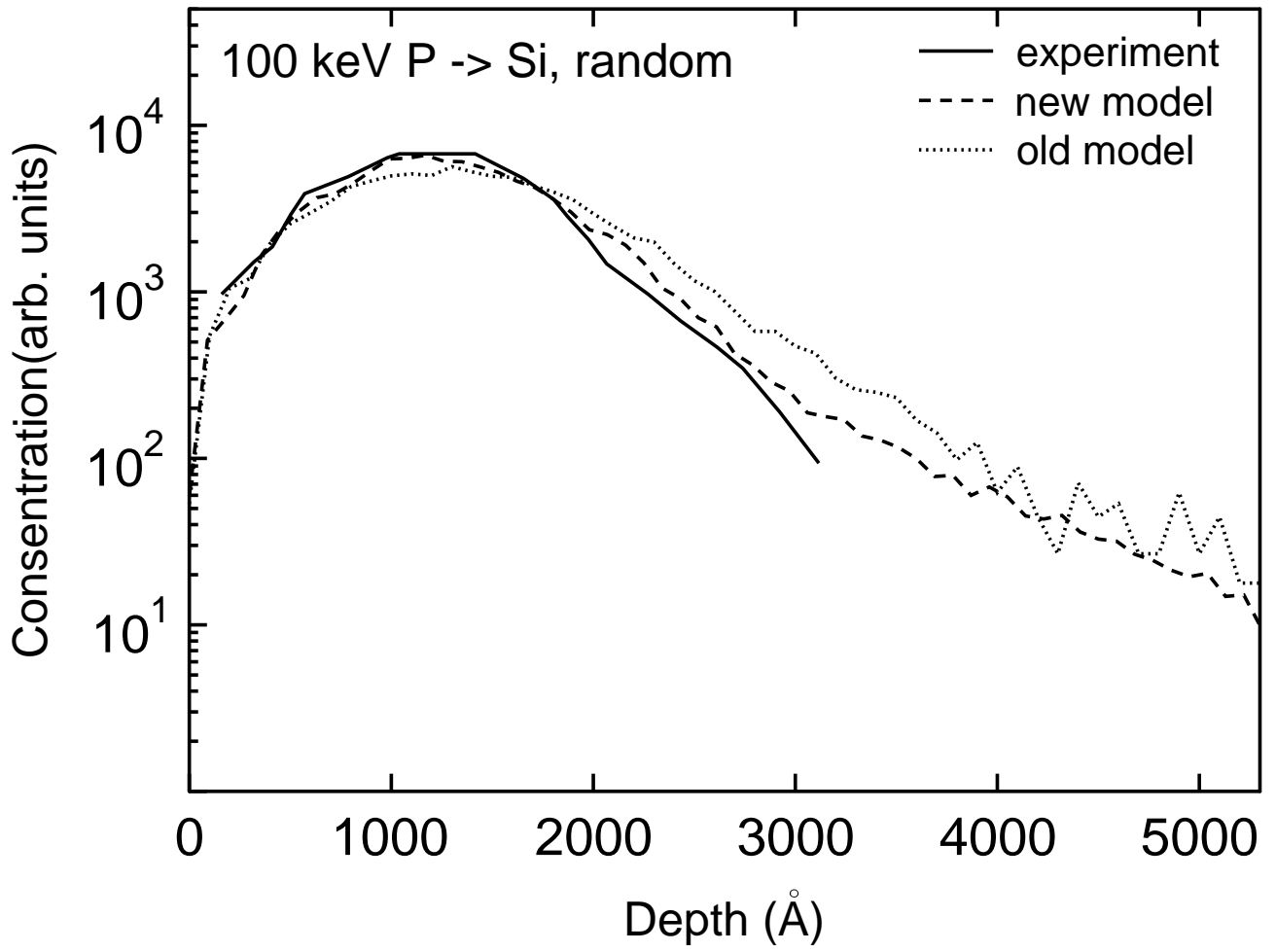
Peltola Fig. 2/12



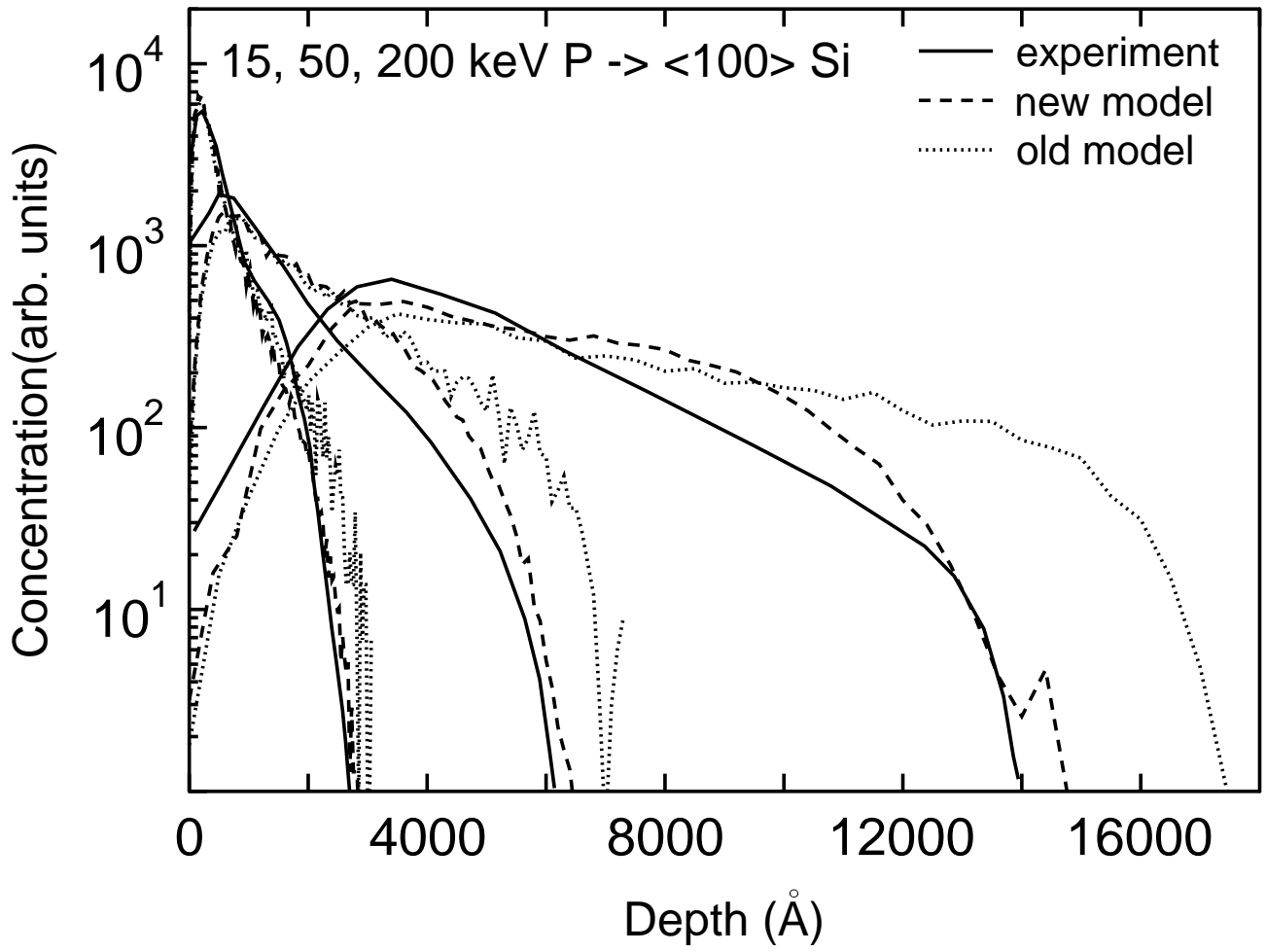
Peltola Fig. 3/12



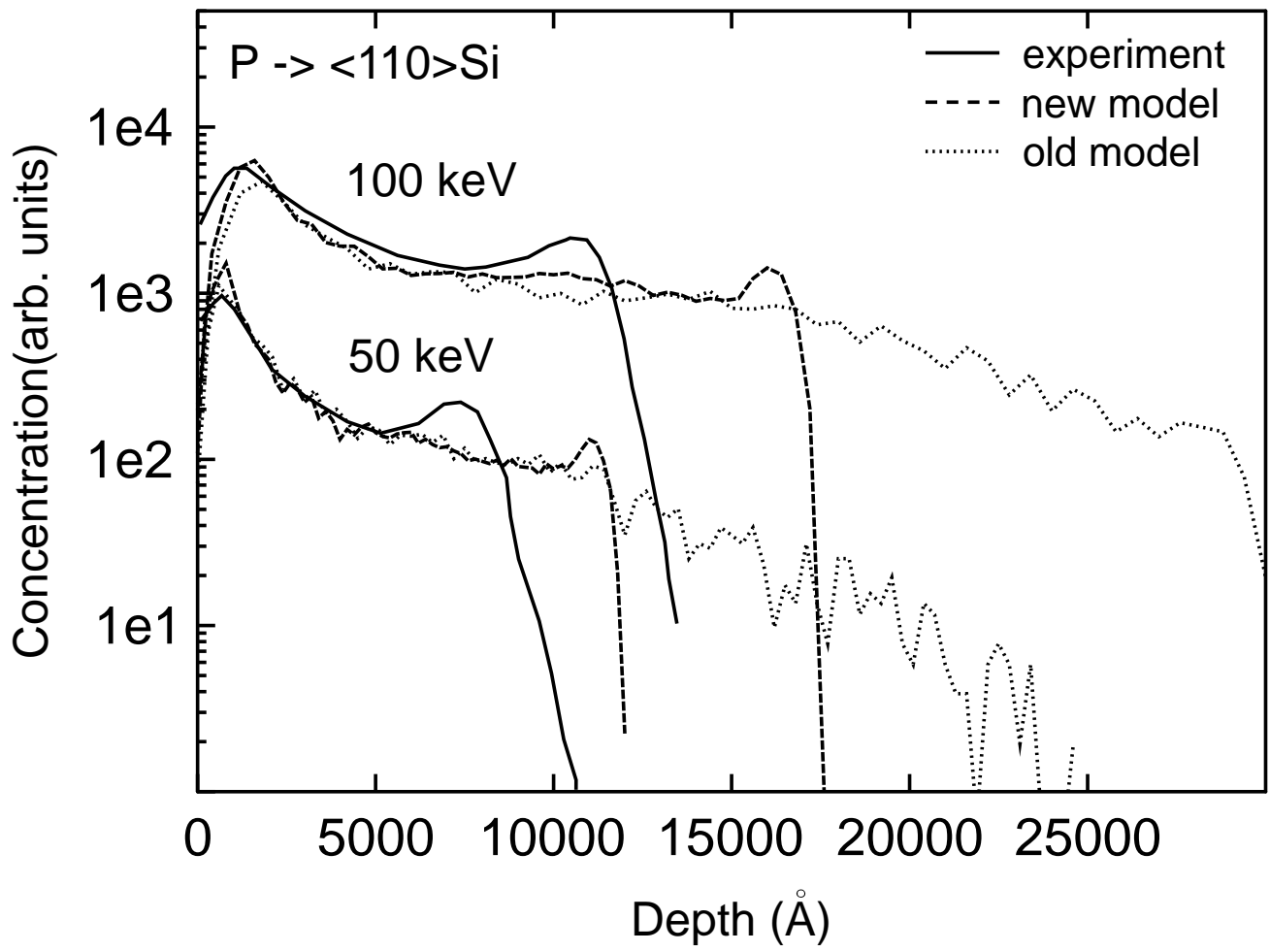
Peltola Fig. 4/12



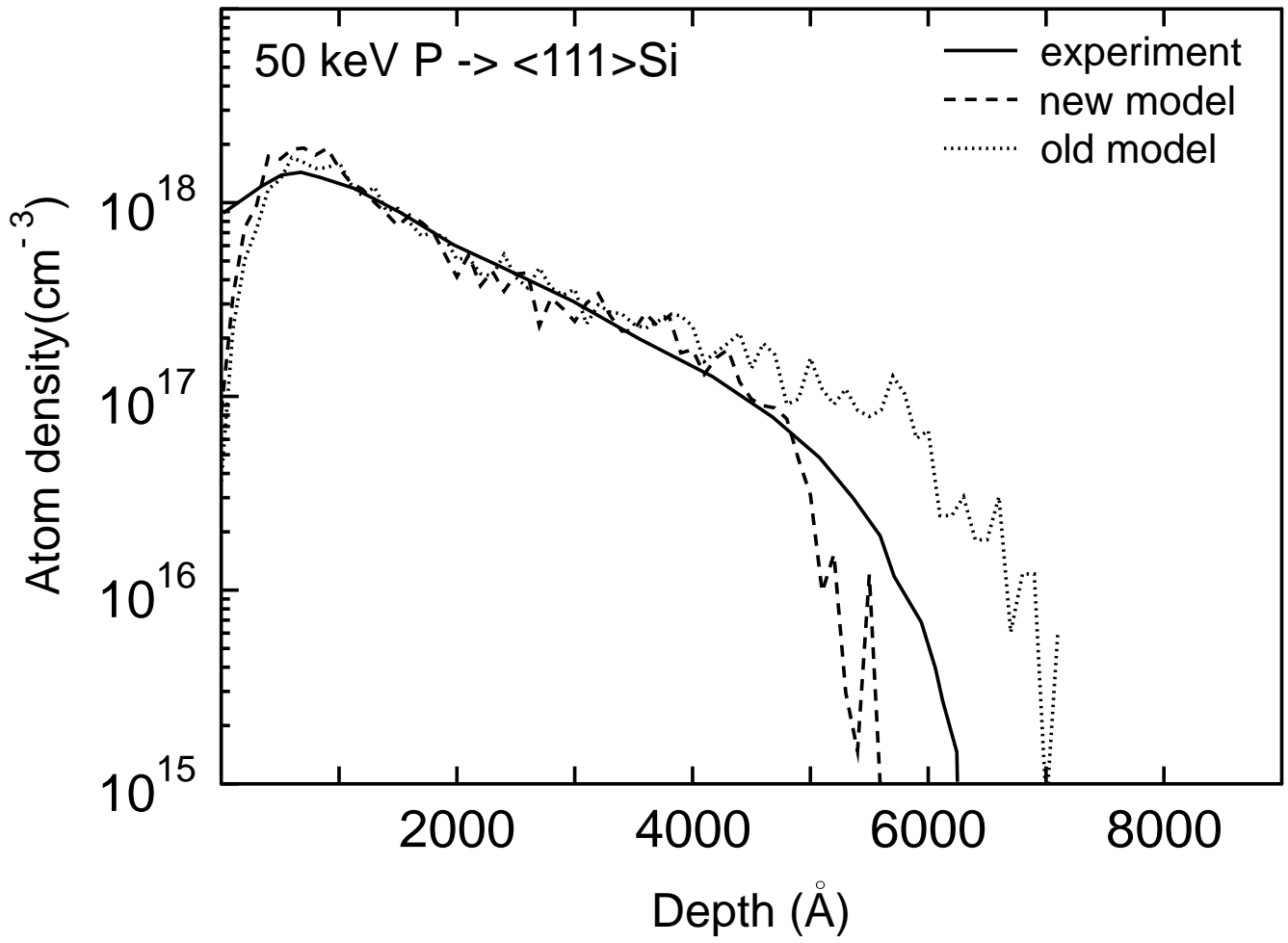
Peltola Fig. 5/12



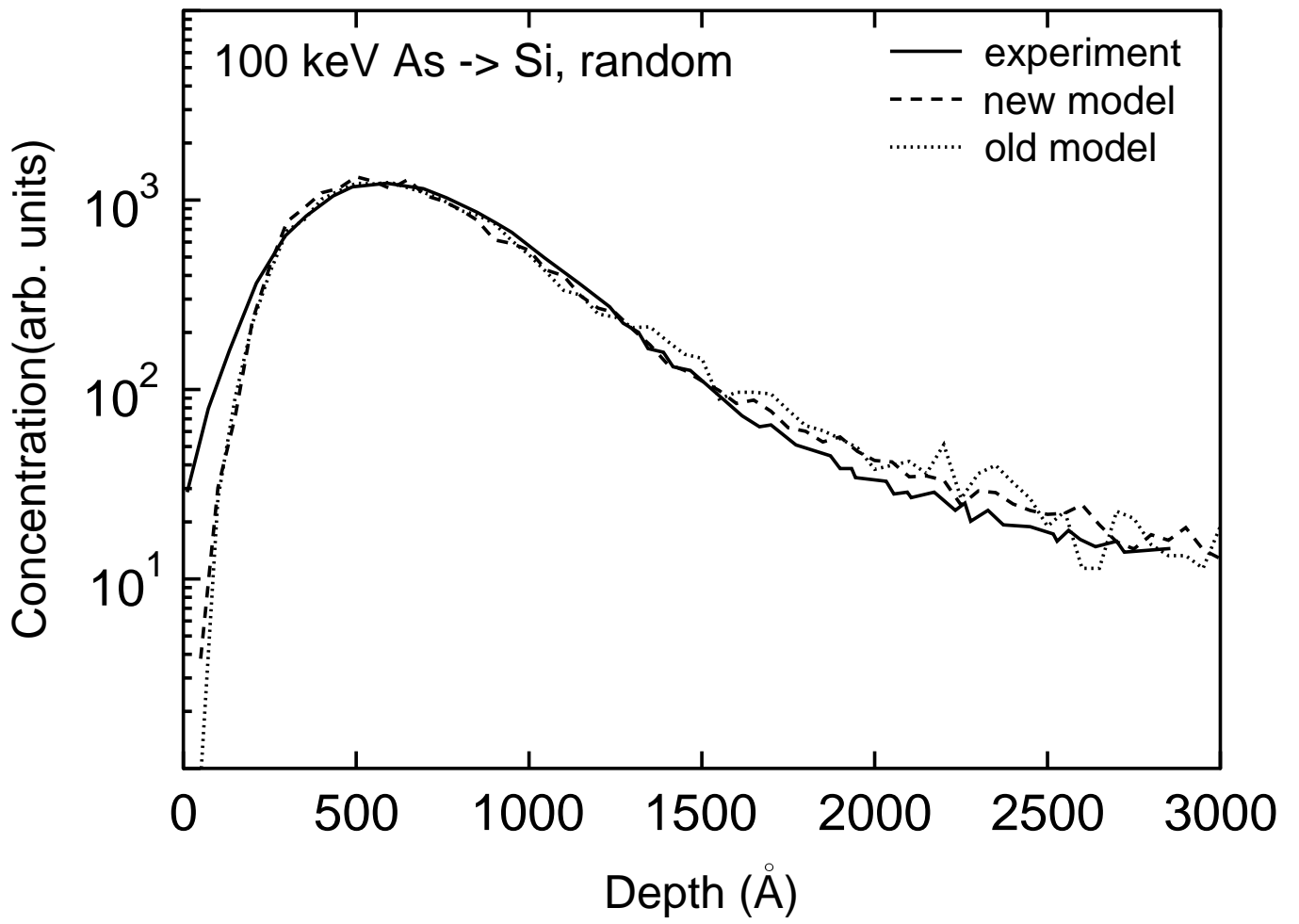
Peltola Fig. 6/12



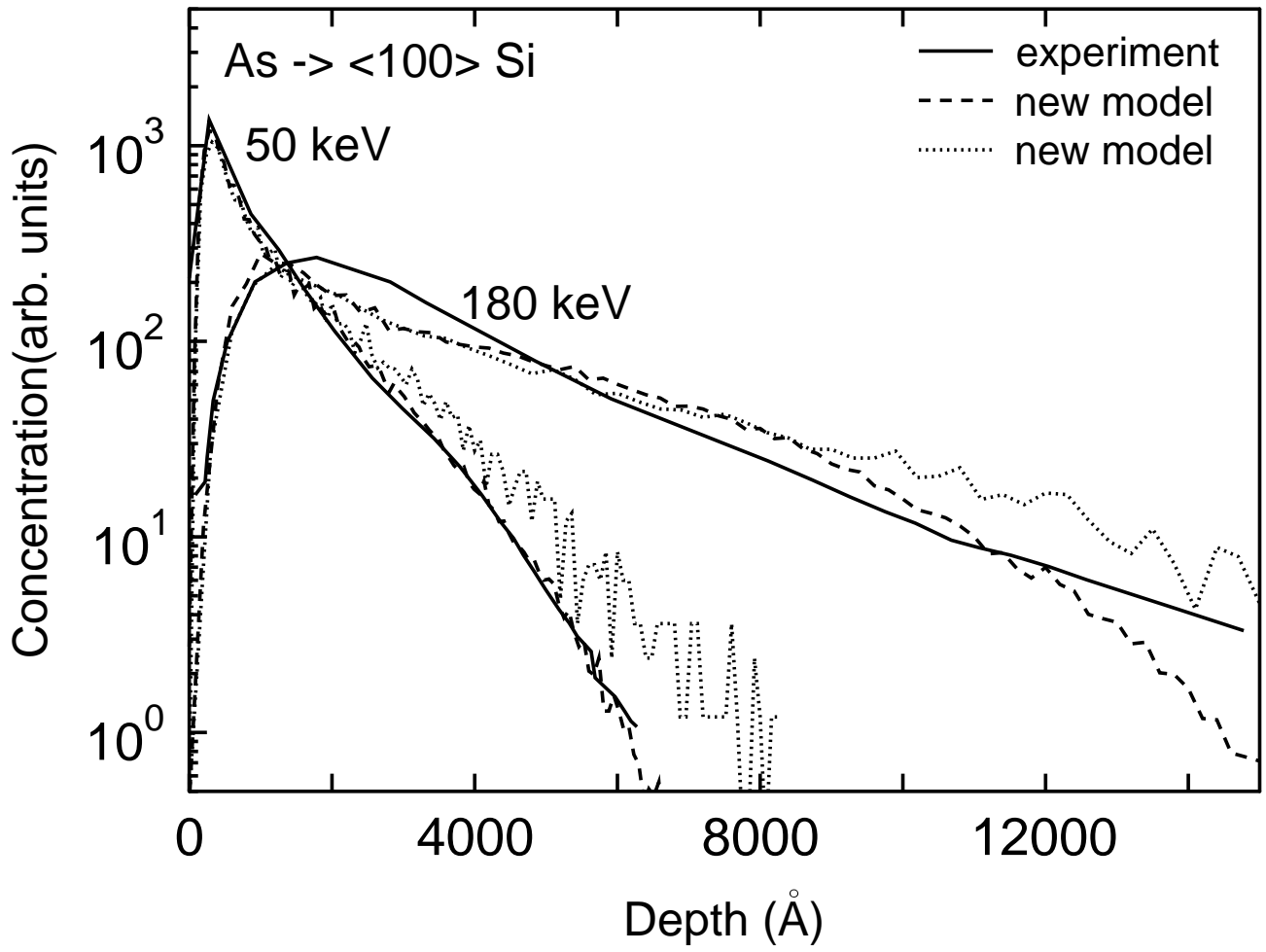
Peltola Fig. 7/12



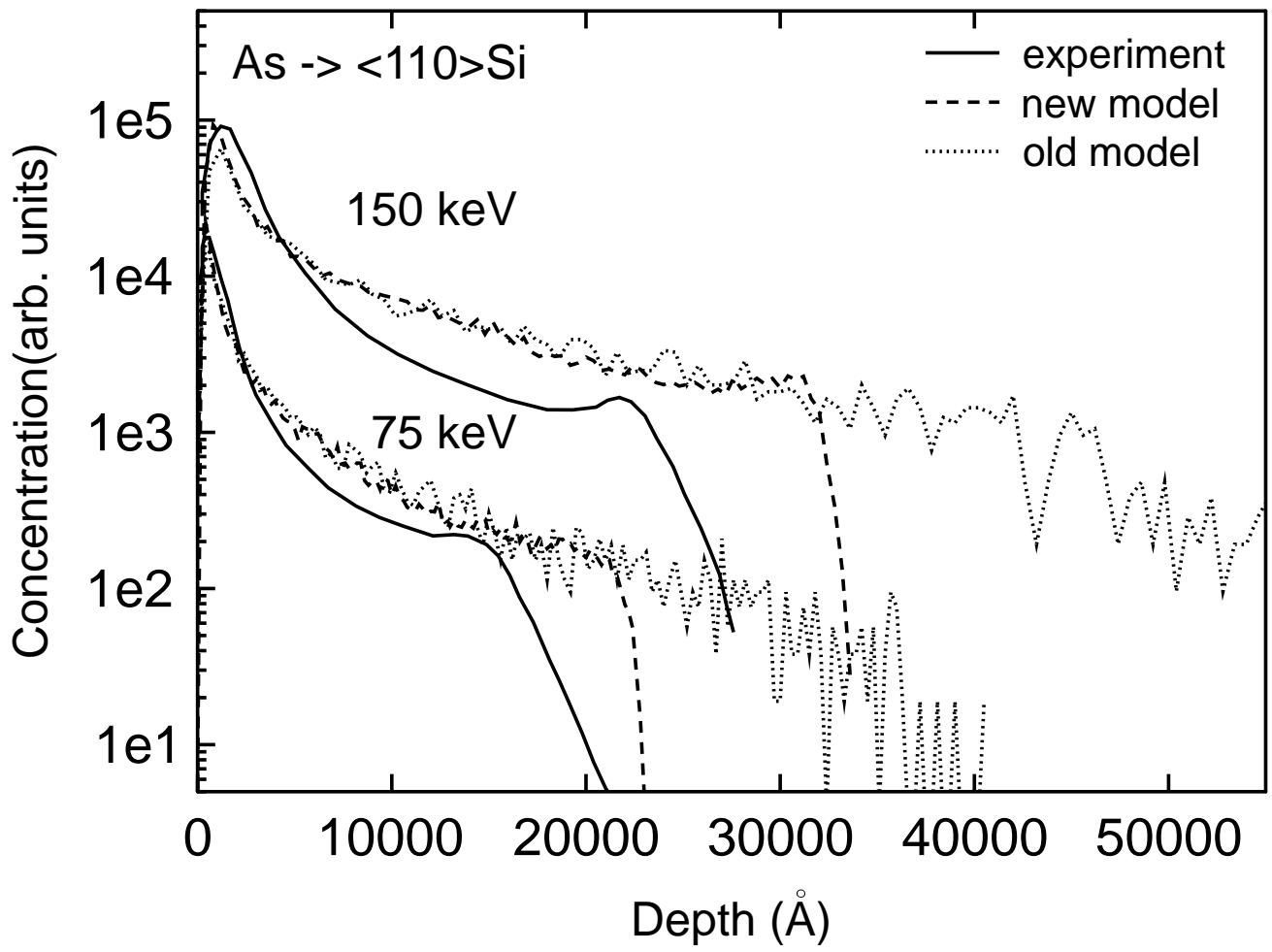
Peltola Fig. 8/12



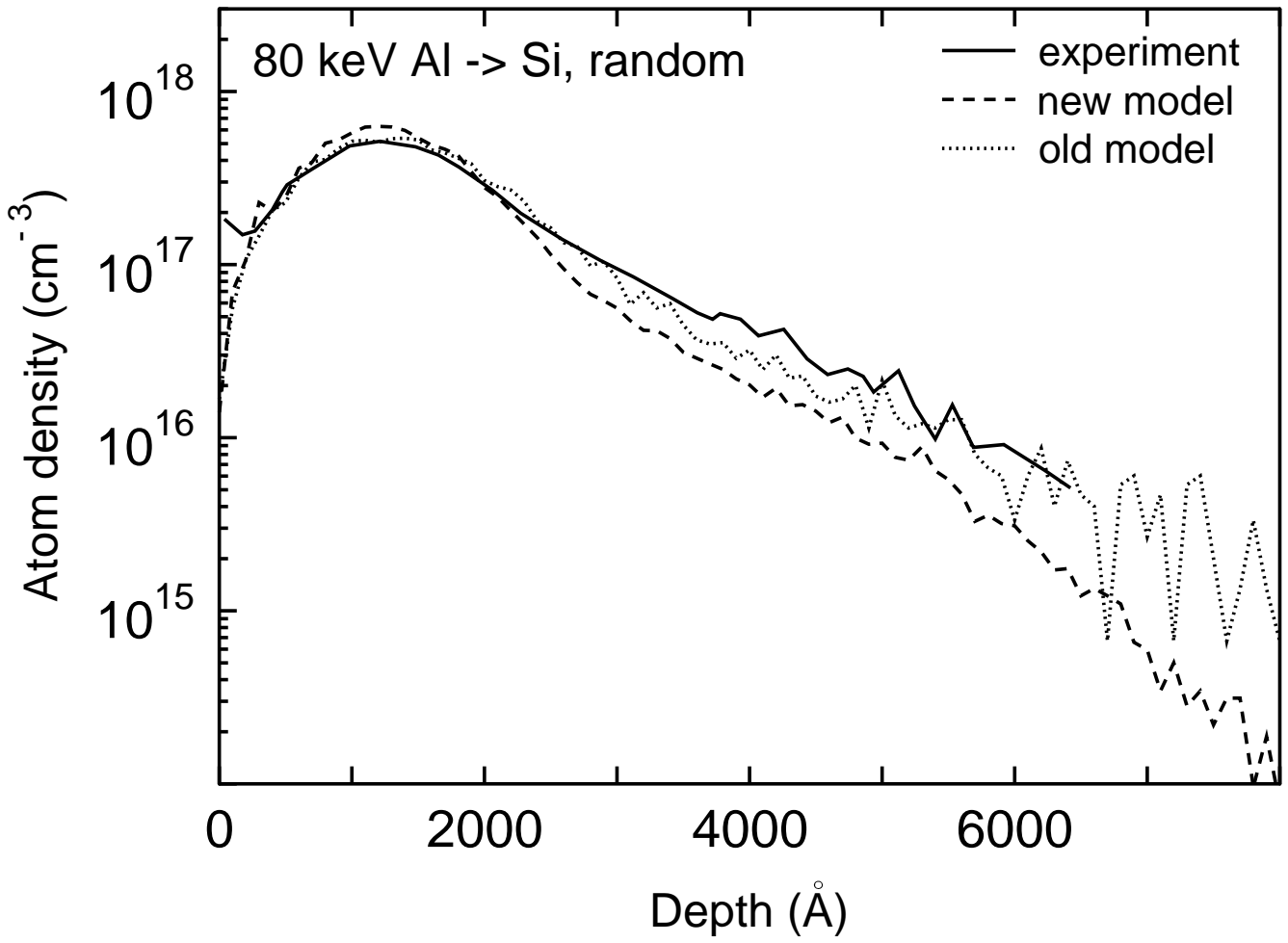
Peltola Fig. 9/12



Peltola Fig. 10/12



Peltola Fig. 11/12



Peltola Fig. 12/12

